Int. J. Exp. Path. (2002) **83**, 67–79

Evidence for a perforin-mediated mechanism controlling cardiac inflammation in *Trypanosoma cruzi* infection

ANDREA HENRIQUES-PONS,*‡ GABRIEL M. OLIVEIRA,* MAURICIO M. PAIVA,* ALEXANDRE F. S. CORREA,* MARCOS M. BATISTA,* RODRIGO C. BISAGGIO,‡ CHAU-CHING LIU,§ VINÍCIUS COTTA-DE-ALMEIDA,* CLAUDIA M. L. M. COUTINHO||, PEDRO M. PERSECHINI‡ AND TANIA C. ARAÚJO-JORGE*

**Laboratório de Biologia Celular – DUBC – Instituto Oswaldo Cruz FIOCRUZ, Rio de Janeiro, Brazil, ‡Laboratório de Imunobiofísica – Instituto de Biofísica Carlos Chagas Filho – UFRJ, Rio de Janeiro, Brazil, §Department. of Medicine – University of Pittsburgh School of Medicine, Pittsburgh, PA, USA, ||Departamento de Biologia Celular e Molecular – UFF, Niterói, Brazil*

Received for publication 10 May 2001
Accepted for publication 08 January 2002

Summary. $CD8^+$ T lymphocytes are considered an important cell population involved in the control of parasitaemia and mortality after *Trypanosoma cruzi* infection. However, despite recent developments in this field, the mechanism whereby this control is exerted is still not completely understood. Here we have used perforin knockout (–/–) mice infected with Y strain *T. cruzi* in order to evaluate specifically the participation of the perforin-based cytotoxic pathway in the destruction of cardiomyocytes, cellular inflammatory infiltration, and control of parasitaemia and mortality. We observed that although parasitaemia was equivalent in perforin (+/+) and (–/–) groups, survival rate and spontaneous physical performance were significantly lower in the perforin deficient mice. The cardiac inflammatory cell infiltration, mostly composed of $CD8^+$ cells, was more evident in perforin (–/–) mice. Ultrastructural and immunofluorescence analysis, as well as plasma creatine kinase activity, revealed cardiomyocyte damage and necrosis, more evident in perforin (–/–) mice. Terminal deoxynucleotidyl transferase-mediated dUTP nick end labelling (TUNEL) assays performed in heart samples revealed similar and modest levels of apoptosis in both perforin (+/+) and (–/–) mice. These results indicate that perforin does not play a pivotal role in the control of parasitaemia and direct lysis of cardiomyocytes, but seems to be an important molecule involved in the control of cardiac inflammation and pathology induced by a highly virulent strain of *T. cruzi*.

Correspondence: Andrea Henriques-Pons, Laboratory Biologia Celular, DUBC, Instituto Oswaldo Cruz, FIOCRUZ, Av. Brazil 4365, Manguinhos, Rio de Janeiro, RJ 21045–900, Brazil. Tel.: 00 55 21 2598 46 37; Fax: 00 55 21 2260 44 34; E-mail: andreah@ioc.fiocruz.br

Keywords: perforin, *Trypanosoma cruzi*, immune regulation, inflammation, myocarditis, infection and cell death

Introduction

Trypanosoma cruzi is the aetiological agent of Chagas' disease, an important infection that affects 16–18 million people in Latin America (TDR, Thirteenth Program Report). Acute infection develops with intracellular proliferation of amastigote forms of *T. cruzi* in different tissues and circulation of free infective trypomastigote forms in the blood. During experimental infection, foci of myocardial cytolysis are detected, with inflammatory cells surrounding both infected and non-infected fibres (Rossi & Bestetti 1995), an observation consistent with what is observed in chagasic patients (Morris *et al*. 1990).

The immunological control *T. cruzi* infection is believed to be mediated by different cell populations, including B lymphocytes (Kumar & Tarleton 1998), T lymphocytes (Da Costa *et al*. 1991), and NK cells (Cardillo *et al*. 1996). Regarding T lymphocytes, mice bearing the disrupted gene of β2-microglobulin (–/–) show significantly higher levels of parasitaemia and mortality when compared to infected (+/–) and (+/+) controls (Tarleton *et al*. 1992). These results are consistent with data obtained with infected mice treated by *in vivo* administration of anti-$CD8^+$ (Tarleton 1990) or anti-$CD4^+$ mAb (Russo *et al*. 1988), mice lacking CD4 and/or CD8 gene expression (Rottenberg *et al*. 1995), thymectomized mice (Schmunis *et al*. 1971) and nude mice (nu/nu) (Da Costa *et al*. 1991). In all approaches used, the mice lacked either peripheral $CD8^+$ or $CD4^+$ T cells, or both, which are believed to play central roles in cytotoxic events and production of pleiotropic interleukins, such as IFN-γ and IL-2.

Recent studies used perforin knockout mice to evaluate the role of $CD8^+$ T cells as effector cells in protection against intracellular protozoa, such as *Toxoplasma gondii* (Denkers *et al*. 1997) and *Trypanosoma cruzi* (Henriques-Pons *et al*. 1998; Kumar & Tarleton 1998; Nickell & Sharma 2000). These papers indicated that perforin-dependent pathways play a limited role in host resistance to these protozoa and suggested that production of IFN-γ is one of the most important elements in this protection.

Perforin is one of the major cytolytic molecules employed by killer cells, such as $CD8^+$ T lymphocytes and NK cells (Young *et al*. 1986). It is packaged into secretory cytoplasmic granules that also contain granzymes and a number of other molecules (Liu *et al*. 1995). Upon contact and specific recognition of target cells, the content of the cytotoxic granules is released into the intercellular space. Perforin then aggregates into large pores inserted into target cell plasma membrane while granzyme B is apparently taken up by receptor-mediated endocytosis (Motyka *et al*. 2001). Although purified perforin can only induce necrosis *in vitro* (Duke *et al*. 1989), the presence of both molecules is required to induce apoptosis of the target cell (Nakajima & Henkart 1994; Trapani *et al*. 1998). Perforin deficient mice specifically lack the perforin-based cytotoxic pathway, maintaining secretory functions, normal distribution of $CD4^+$ and $CD8^+$ T cell subsets, Fas-mediated cytotoxicity and normal patterns of activation and proliferation in response to different pathogens (Cooper *et al*. 1997; Denkers *et al*. 1997; Franco *et al*. 1997).

The study of perforin (–/–) mice infected with a number of different pathogens has revealed that, besides its direct role in target cell killing, perforin is also important in the regulation of peripheral tolerance and autoimmunity (Stepp *et al*. 2000). The lack of a perforin-dependent negative feedback mechanism in the immune response usually correlates with expansion and persistence of activated $CD8^+$ effector T cells *in vivo* and increased susceptibility to infection (Kägi *et al*. 1999; Matloubian *et al*. 1999; Spaner *et al*. 1999).

In the present work, we re-assessed the importance of perforin in the host susceptibility to experimental infection with *T. cruzi* using a highly virulent strain of the parasite. We observed a significantly higher mortality rate, necrotic cardiomyocyte destruction, and more abundant cardiac inflammatory foci, mostly composed by $CD8^+$ T cells, in perforin (–/–) mice. The data indicates that, although perforin may not be directly involved in cardiomyocytes death *in vivo*, it may play an important role in the control of the cellular cardiac inflammatory response, modulating the gathering of inflammatory $CD8^+$ T cells in the cardiac tissue in our findings, suggesting a broader regulatory function for perforin in the immune system.

Materials and methods

Mice

C57BL/6 mice with disrupted perforin gene (perforin (–/–)) (Walsh *et al*. 1994), were bred at the animal facilities of FIOCRUZ. The genotype of the animals was determined

by PCR analysis of the perforin gene using DNA isolated from tail snips as described (Walsh *et al*. 1994). The experiments were carried out with 8-week-old male perforin (–/–) mice and their counterpart (+/+) controls. The FIOCRUZ Committee of Ethics in Research approved the experiments described here, according to resolution 196/96 of the National Health Council of the Brazilian Ministry of Health.

Parasites and infection

Y strain *T. cruzi* was maintained *in vivo* by passage in syngeneic C57BL/6 mice. Blood was collected and trypomastigote forms were isolated as previously described (Araújo-Jorge *et al*. 1989). Thereafter, the parasites were diluted in phosphate-buffered saline (PBS) (Sigma, St Louis, USA), counted in a haemacytometer and the inocula (1×10^4 parasites in 200 μL) then applied by intraperitoneal (ip) injection.

Parasitaemia and mortality

Parasitaemia, expressed as parasites/mL, was evaluated in 5 μL of blood collected from tail snips at the indicated time points, and mortality rate was scored daily. Plasma samples were obtained by centrifugation of 100 μL of blood collected from tail snips in heparinized capillaries, separated by centrifugation, and kept frozen until use.

Spontaneous physical activity

An assay for physical performance was set up using activity wheels (Abelmann 1969). Briefly, mice were adapted to run during three alternate days in periods of 2 h per day. One day before infection, they were allowed to run spontaneously during a 30-min session in order to record the baseline performance of individual mice, expressed in revolutions per session of 30 min (rp 30 min). Each animal was then submitted to the same test on the 8th, 15th, 22nd, 28th, and 35th day post-infection (dpi).

Histopathological and immunohistochemical analysis

Mice were sacrificed 8, 15 and 21/22 days post-infection and processed as described elsewhere (Andrade 1990). Hearts were collected and immediately cryopreserved or fixed in 10% formalin diluted in PBS. Fixed slices were embedded in paraffin and 5 μm thick sections were stained with haematoxylin-eosin. The number of inflammatory foci (composed by $\geq$10 inflammatory cells) and the number of inflammatory cells per focus were determined by scanning the stained tissue slice starting at least 0.5 mm from the tissue edge. The pericardial region was excluded due to difficulties imposed by the excess of inflammatory cells and tissue destruction. The number of parasite nests was determined in the whole tissue and expressed in nests/mm^2. Quantitative analysis was always performed in 10 microscopic fields in each of 2 different slides of heart sections obtained from 3 different mice in each group and time point (a total of 60 individual microscopic fields examined). For phenotypic analysis, 5 μm cryopreserved heart slices incubated with 10% normal goat serum and the samples were stained with anti-CD4 or -CD8 FITC-labelled mAb either on the 21st or 22nd dpi. Actin staining was carried out with 10% phalloidin-FITC (Sigma) diluted in PBS on the 15th dpi. *In situ* apoptosis was accessed on cryopreserved sections collected on the 21st dpi using a FITC-labelled TUNEL assay (Mannhein, Lewes, UK) performed according to the manufacturer's instructions. For *in situ* IFN-γ detection, paraffin was removed from the cardiac sections by heating the slides for 30 min at 60 °C, followed by treatment with xylol and ethanol. The hydrated sections were then washed with PBS for 10 min, incubated with 3% urea for 5 min, and 10% normal goat serum for 30 min. The slides were then washed with PBS for 10 min and incubated for 48 h with anti-IFN-γ (Caltag, San Francisco, USA) at room temperature. After washing overnight, the secondary goat antirat-FITC (Caltag) was added for an additional 1 h and washed with PBS for one hour. Slices were also labelled with the DNA-specific fluorescent dye 4,6-diamidino-2-phenylindole (DAPI) (Sigma) for identification of the nucleus of inflammatory cells.

Ultrastructural analysis

Hearts from normal and infected mice were collected on the 21st dpi and then fixed for 2 h at room temperature with 2.5% glutaraldehyde in 0.1 M sodium cacodylate buffer, pH 7.2. The samples were postfixed for 30 min in a solution containing 1% osmium tetroxide (Merck, Darmstadt, Germany), 0.8% potassium ferricyanide (Sigma), and 5 mM $CaCl_2$ in 0.1 M cacodylate buffer (Sigma), dehydrated in acetone, and embedded in epon (Merck). Ultra-thin sections were recovered in copper grids, stained with 2% aqueous uranyl acetate, and observed under a Zeiss EM-10 (Zeiss, Germany) transmission electron microscope.

IFN-γ quantification

IFN-γ was quantified as previously described (Minoprio *et al*. 1991). Briefly, plates were coated overnight at 4 °C

with R46A2 mAb (originally obtained from DNAX Corp. Palo Alto, CA, USA) and exposed to serially diluted serum samples. Standard curves were simultaneously prepared with known amounts of recombinant IFN-γ (Pharmingen, San Diego, CA, USA). Second step reactions were carried out by incubating the plates with biotinylated AN-18 antibodies and revealed by further incubation with peroxidase-labelled streptavidin. Optical density (od) was scored at 650 nm wavelength in a multi-well plate spectrophotometer (Bio Tek Instruments, Burlington, Vt, USA).

Creatine kinase MB (CK-MB) activity

Heparinized plasma samples collected one day before and on the 8th, 15th and 22nd dpi were analysed for creatine kinase MB (the cardiac isoform of CK) activity using a commercially available kit (Merck), as described elsewhere (Souza *et al*. 2000). This quantitative assay was used as a marker of cardiomyocytes necrotic damage, and the results were expressed as the rate of increase in NADPH (Delta E/min) after 6 sequential readings at 1min intervals at 340 nm in a multiwheel spectrophotometer (BioTek Instruments) at 340 nm.

Statistical analysis

Parasitaemia, spontaneous physical activity and CK-MB levels were compared using the Wilcox non-parametric test. Survival analysis was performed using the Cox-Mantel, Cox-F or Log rank tests. Student's *t*-test was applied for comparing the other parameters. Significant differences were considered when $p < 0.05$.

Results

Course of T. cruzi *infection in perforin (–/–) mice*

To evaluate whether the lack of perforin affects parasitaemia kinetics and mortality rate after infection, perforin (+/+) and (–/–) mice were infected with 1×10^4 trypomastigote forms of Y strain T. cruzi (Fig. 1). There were no significant differences between the parasitaemia of the two groups of mice, as ascertained by the similar latent period, number of circulating parasites, and ability to control parasitaemia to sublatent levels (Fig. 1a). In addition, we have also observed that when chronic mice (6 months post-infection), previously infected with 1×10^2 Y strain parasites, were re-infected with 5×10^5 parasites, both perforin (+/+) and (–/–) mice showed no detectable circulating parasitaemia (data not shown). However, despite the similarities in parasitaemia,

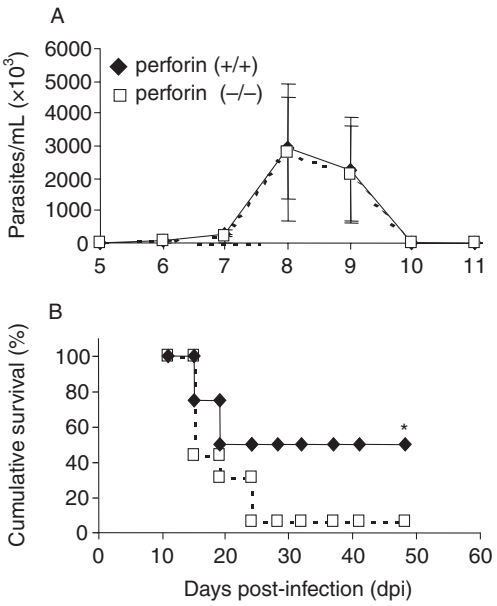

Figure 1. Parasitaemia (a) and survival (b) in perforin (+/+) (closed symbols) and (–/–) (opened symbols) mice infected with 10^4 trypomastigote forms of Y strain *T. cruzi*. The data represents mean $\pm$ standard deviation obtained from at least 8 mice per group. (*) Indicates statistically significant differences ($P < 0.01$) of perforin (–/–) mice as compared to perforin (+/+) mice. Data are representative of 15 experiments.

the survival rate of perforin (–/–) mice was significantly lower than the one of perforin (+/+) mice (Fig. 1b). After approximately 25 days of infection with 1×10^4 parasites, the survival of perforin (–/–) mice was only 0–5%, while in their perforin (+/+) counterparts the survival was 50%. This difference was statistically significant ($P < 0.01$) and represents seven independent experiments with at least 8 mice per group.

Evaluation of physical activity

To investigate possible functional impairments in *T. cruzi*-infected perforin (–/–) mice, an assay for physical activity was carried out by submitting the mice to 30 min sessions of spontaneous exercise on activity wheels (Fig. 2). To perform these experiments, 12-week-old perforin (–/–) mice were used, and the results compared to age-matched non-infected controls. Perforin competent mice showed significantly less spontaneous activity only on the 21st day pi (Fig. 2a), compared to non-infected animals. Surviving mice recovered normal physical activity thereafter. However, perforin deficient mice displayed significantly diminished physical activity after the first week post-infection (Fig. 2b), some time before a decrease in the survival rate could be noticed (Fig. 1b).

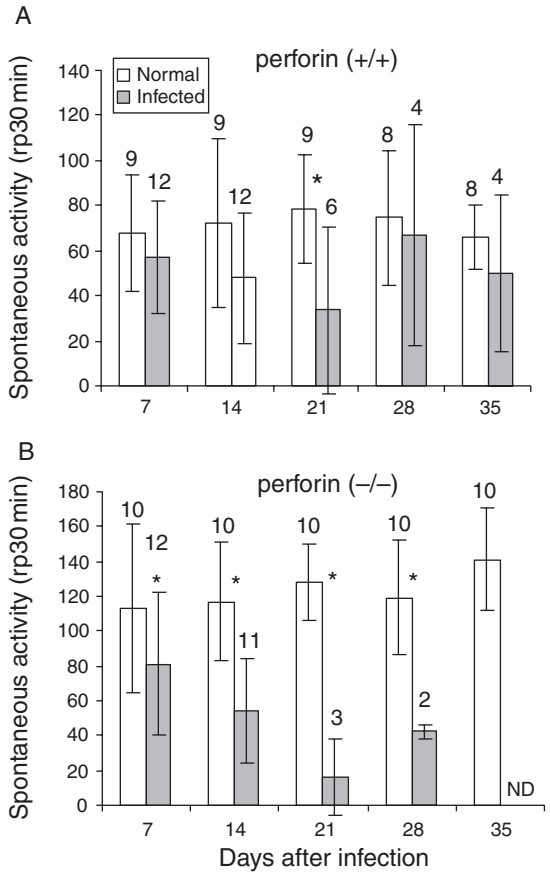

Figure 2. Spontaneous physical activity of normal and infected perforin (+/+) (a) and (–/–) mice (b), infected with 10^4 trypomastigote forms of Y strain *T. cruzi*. Data represent mean ± standard deviation. The number of mice analysed on each day post-infection (indicated upon the bars) decreased due to mortality in the course of infection. (*) Indicates statistically significant differences ($P < 0.05$) of infected mice as compared to non-infected mice.

The *P*-values for infected perforin (–/–) mice when compared to non-infected (–/–) mice on days 7, 14, 21 and 28 pi were 0.02, 0.001, 0.01 and 0.03, respectively.

Histopathological analysis

To study the lower survival rate and the demeaning performance further in the activity test, we investigated the cardiac parasite load and the inflammatory response after infection in perforin (–/–) mice. We first analysed cardiac slices collected on the 8th, 15th and 22nd dpi for the density of parasite nests and the number of infiltrating mononuclear cells (Figs 3 and 4). There was no significant difference between the two groups of mice regarding the frequency of parasite nests (Fig. 3a). A higher frequency of parasitized cardiac fibres was observed on the 8th dpi, corresponding to the peak of circulating parasitaemia (compare Fig. 3a with Fig. 1a), and clearly decreased later. With regard to cellular inflammatory response, we did not find any important cellular infiltration in neither group of mice until the 8th dpi (Figs 3b-c and 4a-b). On the 15th dpi, both perforin (+/+) and (–/–) mice showed increased numbers of inflammatory foci and inflammatory cells per focus (Figs 3b-c and 4c-d), but thereafter perforin (+/+) mice bend to control the cardiac cellular inflammatory response (Figs 3b-c and 4e). In contrast, the perforin (–/–) group displayed inflammatory cell gathering and exuberant foci of inflammation distributed throughout the tissue on the 22nd dpi (Figs 3b-c and 4f).

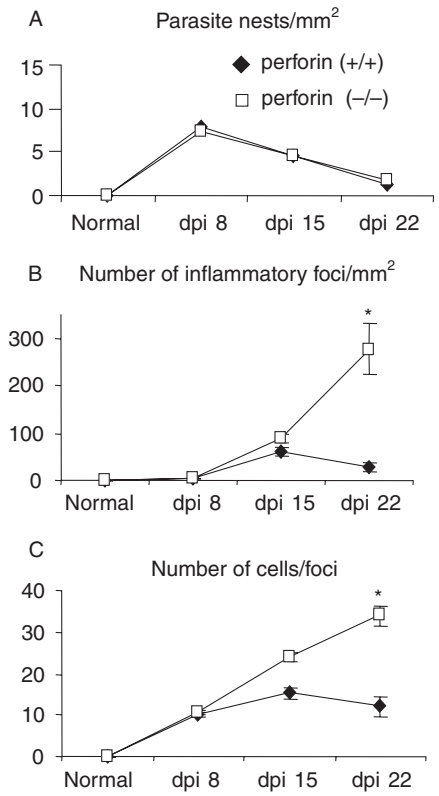

Figure 3. Quantitative analysis of cardiac inflammatory response in perforin (+/+) (closed symbols) and (–/–) (opened symbols) mice infected with 10^4 trypomastigote forms of Y strain *T. cruzi*. The panels represent (a) parasite nests per mm^2 (b) number of foci per mm^2 and (c) number of inflammatory cells per foci. Data are mean ± standard deviation obtained by counting 60 microscopic fields of haematoxilin/eosin-stained heart sections per group and time point. (*) Indicates statistically significant differences ($P < 0.01$) of perforin (–/–) mice as compared to perforin (+/+) mice.

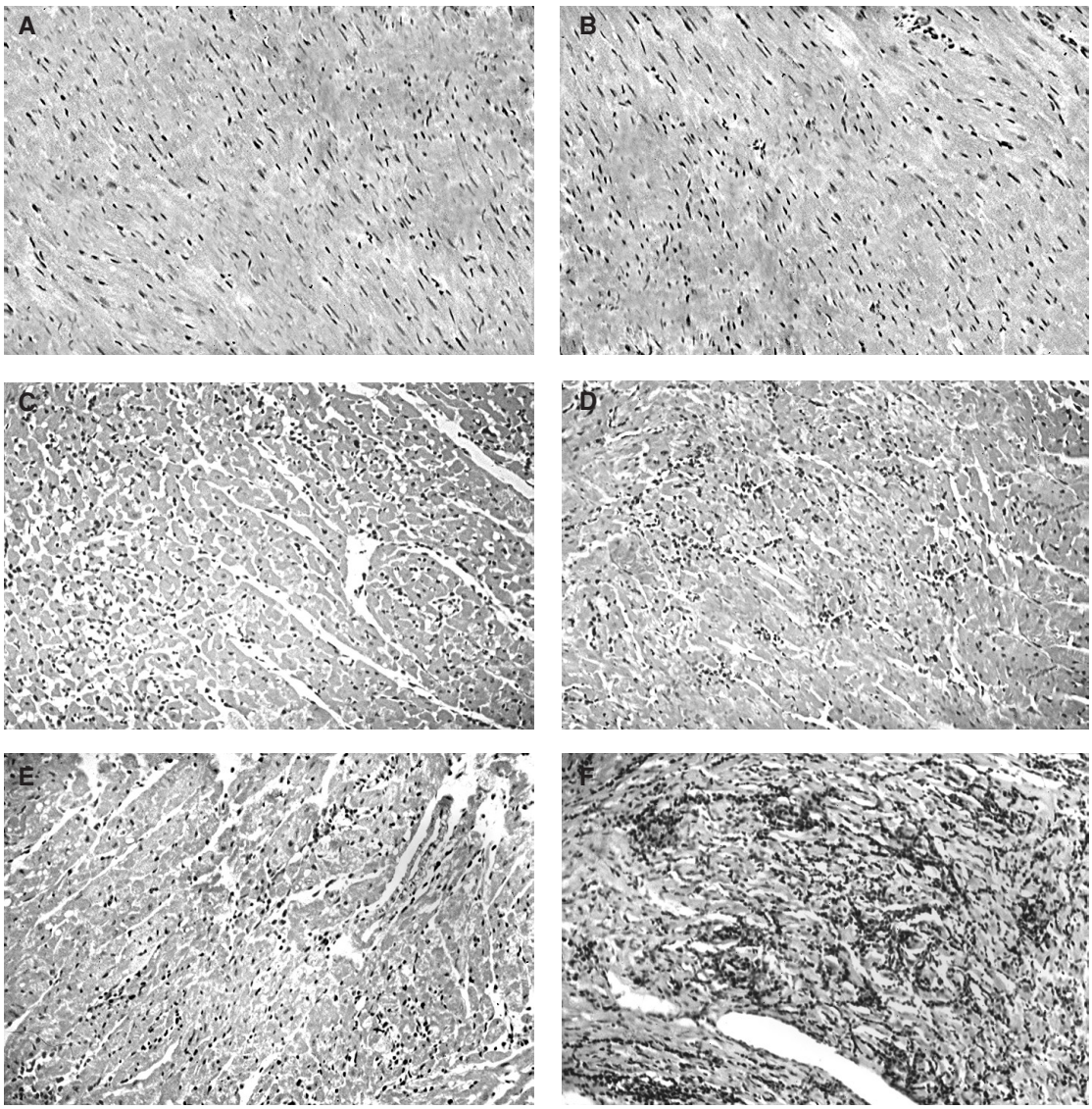

Figure 4. Histopathological analysis of heart in perforin (+/+) (a, c and e) and (–/–) mice (b, d and f). Hematoxilin/eosin-stained heart sections were taken after 8 (a and b), 15 (c and d), and 22 (e and f) days post infection with Y strain *T. cruzi*. The original magnification was 160×.

The phenotypic analysis of cardiac inflammatory cells performed with anti-CD4 or -CD8 mAb indicated an early and modest migration of $CD4^+$ cells to the heart from the 8th to the 15th dpi, in both groups of infected mice (data not shown). However, from the second to the third week of infection, those cells were replaced by $CD8^+$ cells, which composed most of the inflammatory foci thereafter in both perforin (+/+) and (–/–) mice (Figs 5a-c).

IFN-γ production

$CD8^+$ T cells are important producers of IFN-γ, and this cytokine plays a pivotal role in the resistance of *T. cruzi* infection, inducing macrophages activation and destruction of intracellular parasites (Cardillo *et al*. 1996). However, at higher levels, this cytokine can also induce cardiomyocytes death (Shimojo *et al*. 1999; Melino *et al*. 2000). Therefore we decided to evaluate the plasma levels IFN-γ during the first two weeks of infection (Fig. 6) and the presence of IFN-γ-producing cells in the heart on the 21st dpi (Fig. 7). Perforin (+/+) infected mice displayed a peak of plasma IFN-γ on the 8th dpi that returned to normal levels on the 15th dpi (Fig. 6), and IFN-γ-producing cells were rarely found in the myocardial infiltrations of these mice on the 21st dpi (Fig. 7a-b). Perforin (–/–) infected mice

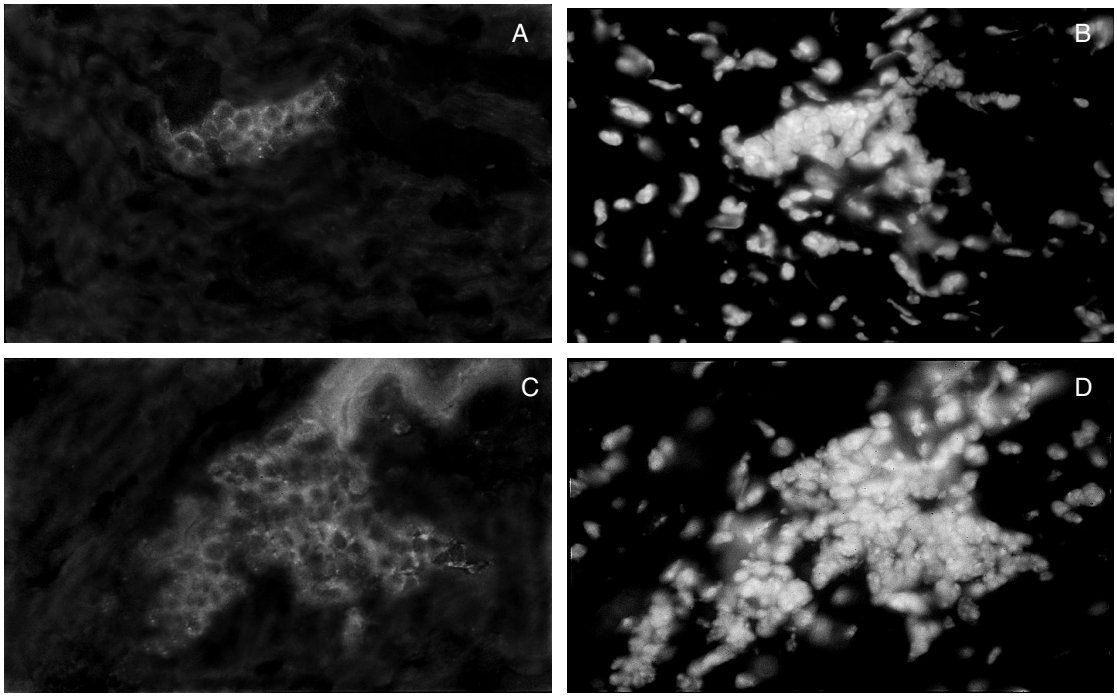

Figure 5. Immunofluorescence labelling of $CD8^+$ cells (a and c) and DNA staining with DAPI (b and d) in cardiac inflammatory foci of perforin (+/+) (a and b) and (–/–) mice (c and d) after 22 days of infection with Y strain *T. cruzi*. The original magnification was 630×.

also displayed increased levels of plasma IFN-γ on the 8th dpi, but, in contrast to the perforin (+/+) group, this value remained high on the 15th dpi (Fig. 6). In addition, high numbers of IFN-γ-producing inflammatory cells were observed in the myocardial tissue on the 21st dpi (Fig. 7c-d).

Myocardial destruction

We then evaluated the pattern of cardiomyocyte death and whether the destruction of these cells was involved

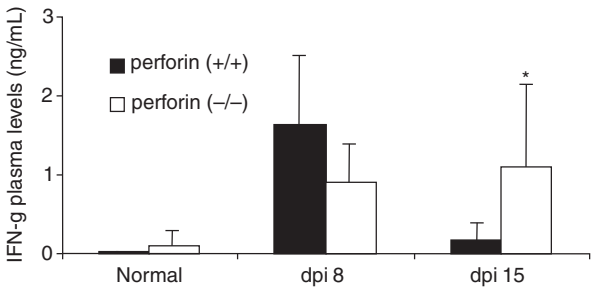

Figure 6. Quantification of plasma levels of IFN − γ in perforin (+/+) (closed bars) and (–/–) (opened bars) mice before infection and after the 8th and 15th dpi with Y strain *T. cruzi*. (*) Indicates statistically significant differences ($P < 0.05$) of perforin (–/–) mice as compared to perforin (+/+) mice.

in the higher susceptibility of perforin (–/–) mice to the infection. TUNEL assay performed on the 21st dpi showed that both perforin (+/+) and (–/–) mice displayed small and similar pattern of apoptosis (Fig. 8). Plasma CK-MB activity, a myocardial marker of cell damage (Souza *et al*. 2000), was measured to quantify cardiomyocyte cell death through necrotic pathways (Fig. 9). Significantly higher levels of CK-MB activity was observed in perforin (–/–) infected mice on the 15th dpi when compared to perforin (+/+) mice on the same time-point ($P < 0.05$) (Fig. 9). These results correlate with the levels of cardiac inflammation observed in Fig. 3 and indicate that there is an increase in cardiomyocyte necrotic cell death in the course of the inflammatory process in perforin deficient mice.

To further evaluate cardiomyocyte damage, we labelled heart slices with the actin-specific fluorescent dye phalloidin-FITC (Fig. 10). Cytoskeletal disarrange and loss of cardiomyofibres integrity surrounded by inflammatory foci was clearly more evident in perforin (–/–) mice (Fig. 10c-d) when compared with perforin (+/+) mice (Fig. 10a-b). To better characterize the pattern of destruction of cardiomyocyte, transmission electron microscopy analysis was performed in cardiac tissues of perforin (–/–) mice on the 21st dpi (Fig. 11). We observed extensive areas with apparent destruction

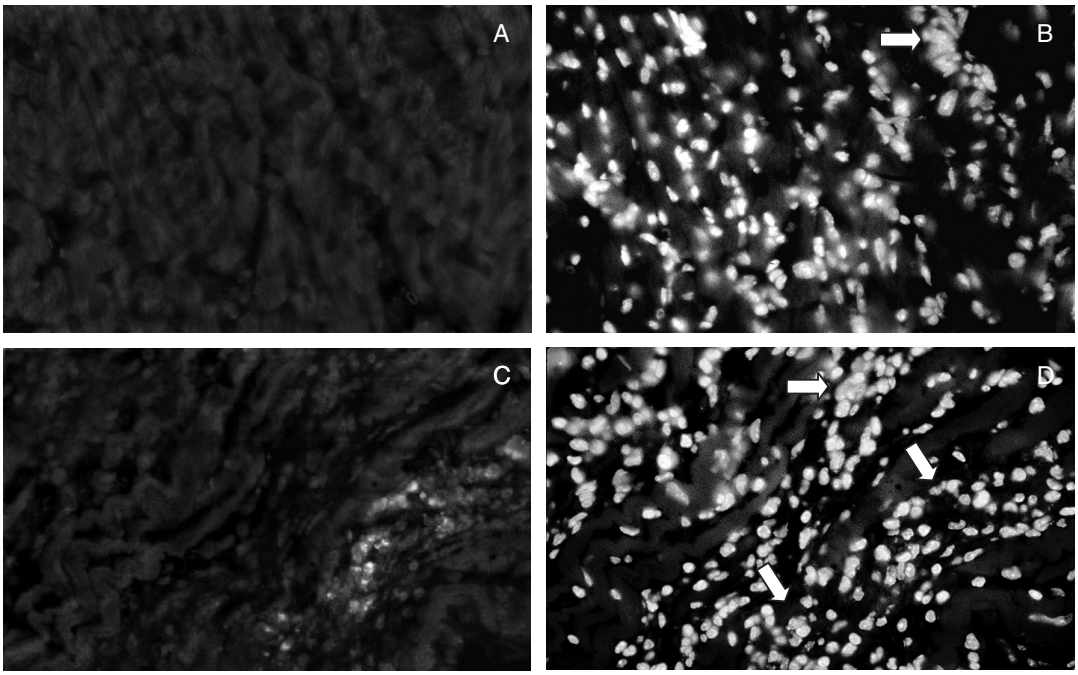

Figure 7. Immunofluorescence detection of inflammatory IFN-γ-producing cells in paraffin-embedded heart sections taken from perforin (+/+) (a) and (–/–) (c) mice after 21 days of infection with Y strain *T. cruzi*. Nuclear labelling with DAPI corresponding to the same microscopic fields are also shown in (b) and (d), respectively. Arrows indicate inflammatory infiltrates. The original magnification was 630×.

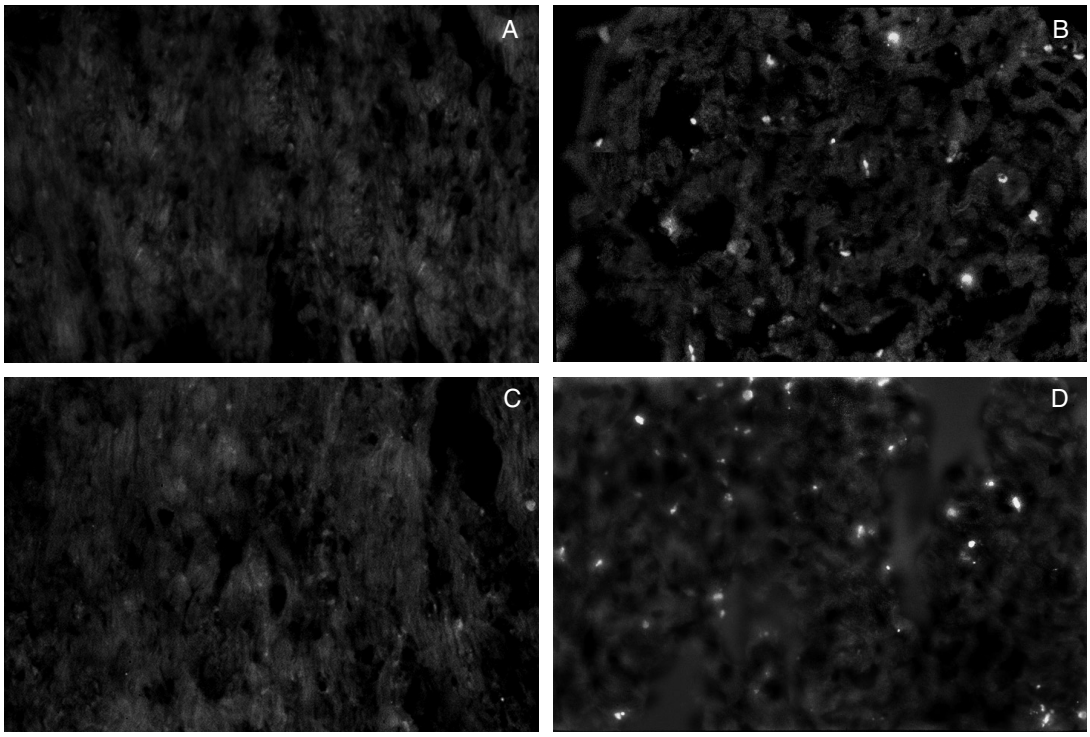

Figure 8. Apoptosis detection by TUNEL-FITC in cryopreserved heart sections taken from normal (a) or infected (b) perforin (+/+) mice and from normal (c) or infected (d) perforin (–/–) mice on the 21st dpi. The original magnification was 630×.

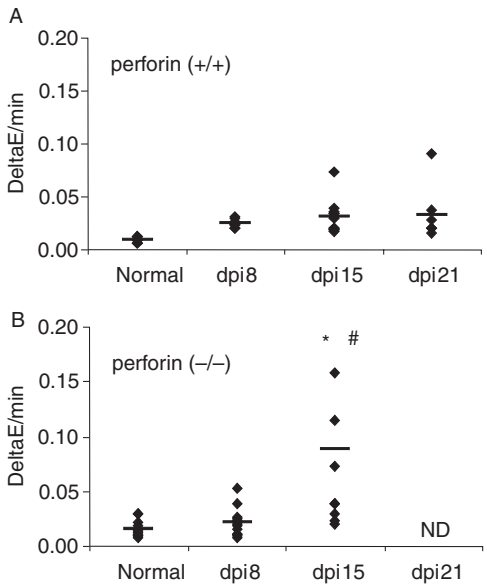

Figure 9. Quantification of CK-MB activity in plasma taken from perforin (+/+) (a) and (–/–) (b) mice before and after 8, 15 and 22 days of infection. Solid lines represent the median of individual groups and the dots indicate individual mice values. (ND) The corresponding CK-MB dosages were not included because most of the perforin (–/–) mice died before the 21st dpi. (*) Indicates statistically significant differences ($P < 0.05$) of perforin (–/–) mice as compared to perforin (+/+) mice. (#) Indicates statistically significant differences ($P < 0.05$) of infected perforin (–/–) mice on the 15th dpi as compared with control (–/–) mice.

of cytoskeleton and loss of organization of the highly structured myofibrils typical of normal myocardium. In addition, we have also observed swollen and collapsed patterns of mitochondria morphology. We found no direct association between myofibrils derangement and abnormal mitochondria.

Discussion

It has already been shown that T lymphocytes, and particularly $CD8^+$ T cells, play an important role in the control of *T. cruzi* infection (Schmunis *et al*. 1971; Da Costa *et al*. 1991; Rottenberg *et al*. 1995; Tarleton 1990). However, since most of the previous studies were based in the depletion of peripheral T cell subsets, the participation of perforin in the destruction of cardiomyocytes and morbidity was not clear. The use of perforin (–/–) mice allowed us and others investigate specifically the perforin-based cytotoxic pathway (Kumar & Tarleton 1998; Walsh *et al*. 1994; Nickel & Sharma 2000). In this regard, it is worth noting that besides target cell lysis, perforin has also been involved in the control of activated $CD8^+$ T cell population by an unknown mechanism (Stepp *et al*. 2000; Sambhara *et al*. 1998; Spielman *et al*. 1998; Matloubian *et al*. 1999; Spaner *et al*. 1999). Moreover, despite the clear participation of perforin-mediated cytotoxicity in many important events (Van den Broek *et al*. 1996; Kägi *et al*. 1994), some cases were described in which perforin is not apparently required to control infection, such as mycobacterial infection (Cooper *et al*. 1997), rotaviruses (Franco *et al*. 1997), primary rejection of some allografts (Walsh *et al*. 1996) and some cytophatic and non-cytophatic viruses (Kägi *et al*. 1995). In addition, a direct role for perforin in parasite destruction does not seem to be the case, since the purified protein is unable to form pores and kill *T. cruzi* in *in vitro* assays (Bisaggio *et al*. 1997).

Therefore, the participation of $CD8^+$ T cells in the control of the infection could be conveyed by at least three basic mechanisms: (1) direct destruction of infected cells by either a perforin-dependent or independent mechanism such as fas/fas–L interaction; (2) secretion of pleiotropic cytokines; and/or (3) perforin-dependent negative feedback on activated $CD8^+$ T cells.

Our results show that, in regard to parasite load, perforin (–/–) mice did not differ from their (+/+) counterpart in the ability to control circulating parasitaemia after infection with Y strain *T. cruzi*, as originally described for the Brazil strain of the parasite (Kumar & Tarleton 1998). Furthermore, the time course of the control of parasitaemia suggests that cognate immune response is also not involved during this stage of infection as studies performed with RAG (–/–) mice showed that the contribution of this type of immune response becomes apparent only by day 14 of infection (Abrahamson & Coffman 1996). In accordance with this hypothesis, we have not detected significant differences between perforin (+/+) and (–/–) mice when they were infected with the clone Dm28c, a model in which detectable parasitaemia develops only after two weeks of infection (Henriques-Pons *et al*. 1998). These results demonstrate that perforin is not a central molecule employed either by innate or by specific immune responses to control the parasite load of the acute phase. These findings called our attention to the importance of cytokines production by $CD8^+$ T cells in the control of parasitaemia. In addition, Denkers and collaborators (Denkers *et al*. 1997) found that vaccinated perforin (–/–) mice are completely resistant to challenge with a virulent strain of *T. gondii*. These authors attributed this result to IFN-γ production, which remained unimpaired in the perforin (–/–) mice.

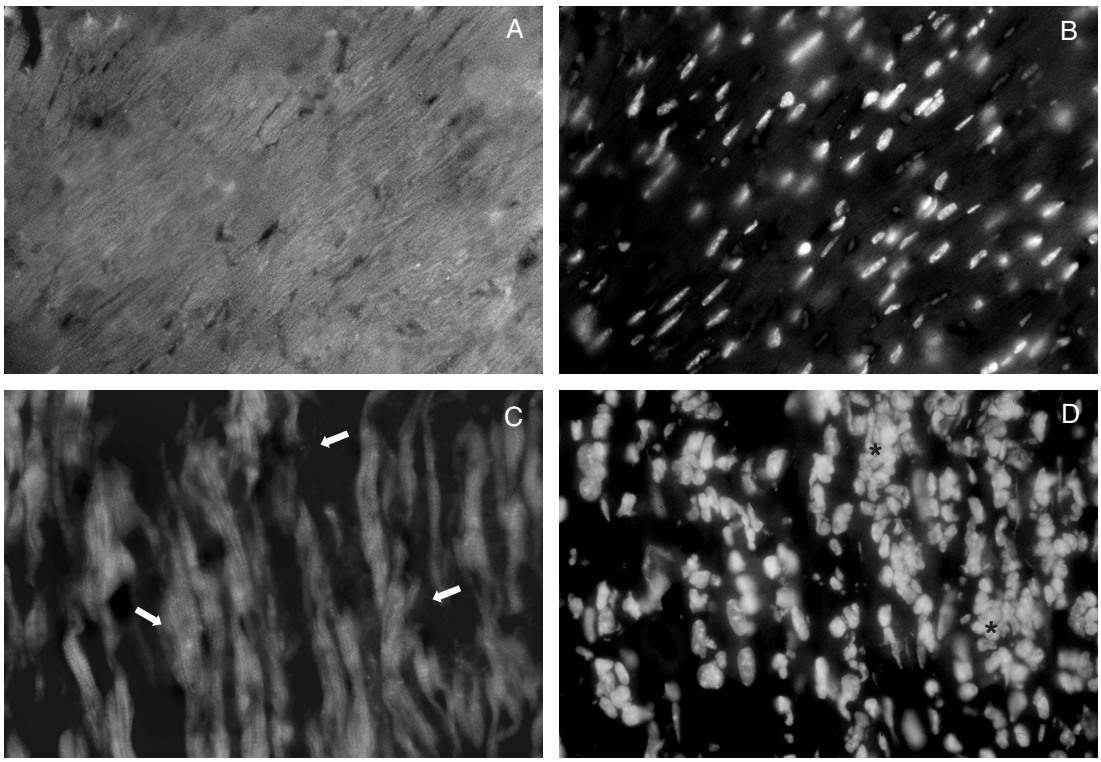

Figure 10. Actin labelling with phalloidin-FITC in cryopreserved heart sections taken from normal (a-b) or infected perforin (–/–) mice (c-d) on the 15th dpi. Nuclear labelling with DAPI corresponding to the same microscopic fields of (a) and (c) are shown in (b) and (d), respectively. The original magnification was 630×. Arrows indicate some points of cardiomyocytes destruction and (*) indicate inflammatory infiltration.

The infection with Y strain *T. cruzi* displayed a higher rate of mortality in perforin (–/–) when compared to (+/+) mice, although another group has observed no differences in the susceptibility after infection with the Brazil strain of *T. cruzi* (Kumar & Tarleton. 1998). The data illustrates the complex variation of resistance and immunological interactions of the different models used to study parasite infections.

The histopathological analysis showed that both groups of infected mice had intense cardiac damage, mainly through non-apoptotic pathways, as ascertained by plasma CK-MB activity, cytoskeletal labelling, TUNEL assays, and ultrastructural analysis. The data indicates that although $CD8^+$ T cells represent most of the inflammatory infiltrates, perforin does not directly induce destruction of myocardial fibres. We also found a much stronger cardiac inflammatory response, with more abundant and exuberant inflammatory foci in the perforin-deficient mice from the 15th dpi on. This suggests that perforin may be somehow involved in the restrain of the cellular cardiac inflammatory response after *T. cruzi* infection. This hypothesis is in agreement with recently connoted functions of perforin in the regulation of the immune response (Sambhara *et al*. 1998; Spielman *et al*. 1998; Matloubian *et al*. 1999; Spaner *et al*. 1999; Stepp *et al*. 2000). These include down-regulation of Ig production, regulation of autoimmunity and cytotoxic T lymphocyte responses to some viral infections, and, possibly, activation-induced cell death (AICD) of cytotoxic T lymphocytes. It could be possible that in *T. cruzi*-infected perforin-competent mice, perforin-producing cytotoxic cells were recognizing and destroying infected inflammatory-recruiting cells in the cardiac tissue, such as macrophages, thus reducing the migration of new inflammatory cells after two weeks of infection. In the absence of perforin, these recruiting cells would still be present and stimulating the inflammation. A similar hypothesis has been suggested in other situations (Stepp *et al*. 2000), and is under investigation in our laboratory.

Our results demonstrated cardiomyocytes damage determined by perforin-alternative pathway(s). It is possible that IFN-γ, locally secreted by the abundant cardiac inflammatory cells observed in infected perforin (–/–) mice were inducing cardiomyocytes necrosis (Pulkki 1997). In accordance with this hypothesis, the infected

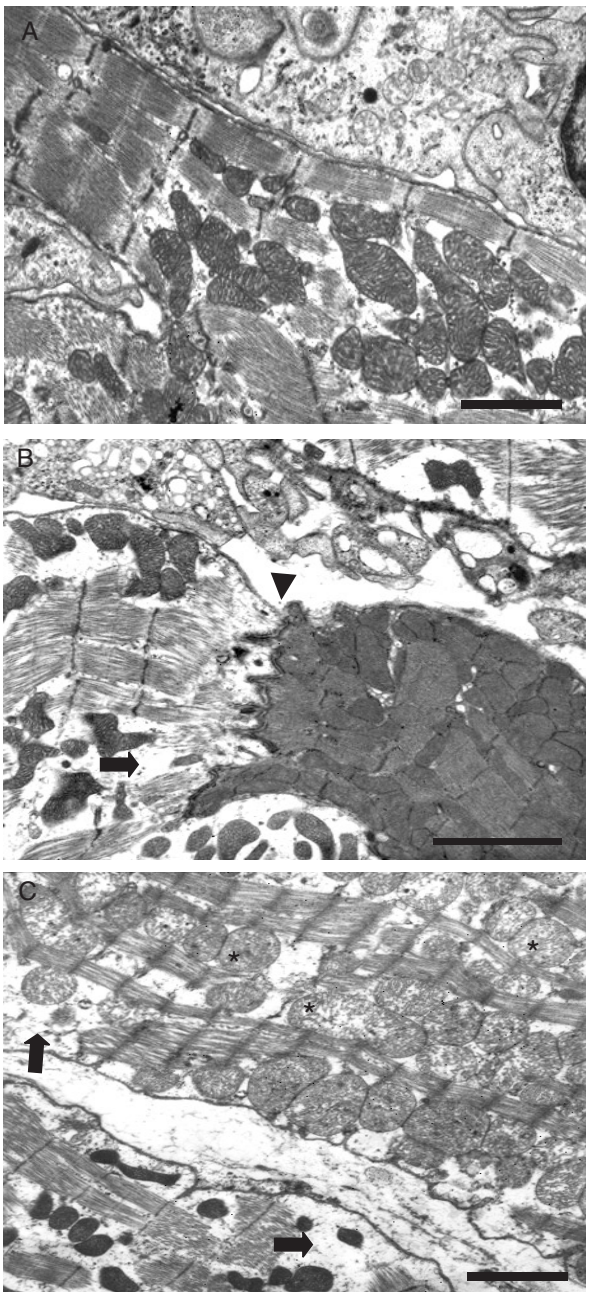

Figure 11. Electron microscopic analysis of cardiac tissue samples performed in infected perforin (–/–) mice collected on the 21st dpi. (a) Normal morphology; (b-c) Some damaged mitochondria (*), disarranged cytoskeleton (arrow). The arrowhead in (b) indicate, and an intercalar disc between a damaged (left) and an apparently normal fibre (right).

perforin-deficient mice displayed higher plasma levels of IFN-γ after the 15th dpi and also more IFN-γ-producing cells in the cardiac inflammatory foci on the 21st dpi, when compared to the infected (+/+) counterparts. In spite of the clear role of IFN-γ as a protective cytokine in different pathologies, such as *Leishmania major* (Scharton-Kersten & Scott 1995), *T. gondii* (Walker *et al*. 1997) and *T. cruzi* (Cardillo *et al*. 1996), it is possible that overproduction of this cytokine can induce the death of cardiomyocytes (Reed 1998; Shimojo *et al*. 1999). Moreover, inflammatory cells gathered in the cardiac tissue of deficient mice could inflict direct damage to the cardiomyocytes. Cardiomyocytes have altered plasma membranes and remarkably increased permeability at the site of contact or close opposition with macrophages in experimental *T. cruzi* myocarditis (Rossi & Silva 1990).

In conclusion, we demonstrated that the perforin-based cytotoxic pathway can modulate the cellular inflammatory response in the cardiac tissue after *T. cruzi* infection. However, perforin does not seem to be involved in the destruction of cardiomyocytes or in the control of circulating and cardiac parasite load observed in the acute phase of the infection.

Acknowledgements

We are grateful to Joel Majerowiks for helping in the establishment of the knockout mice colony. We also would like to thank Solange Lisboa de Castro for critical reviews of the manuscripts, Paola Minoprio and Alain Cosson for helpful support in cytokine quantification, and Bianca Perdigão Olivieri and Cleber da Silva Marques for helpful support during the experiments.

Funding

This work was financed by grants from Conselho Nacional de Desenvolvimento Científico e Tecnológico do Brazil (CNPq), Programa de Núcleos de Excelência (Pronex), Financiadora de Estudos e Projetos (FINEP), Fundação de Amparo à Pesquisa do Estado do Rio de Janeiro (FAPERJ), Fundação Oswaldo Cruz (Papes-FIOCRUZ), and Fundação Universitária José Bonifácio (FUJB/UFRJ).

References

Abelmann W.H. (1969) Experimental infection with *Trypanosoma cruzi* (Chagas' disease): a model of acute and chronic myocardiopathy. *Ann. N.Y. Acad. Sci.* **156**, 137–151.

Abrahamson I.A. & Coffman R.L. (1996) *Trypanosoma cruzi*: IL-10, TNF, IFN-γ, and IL-12 regulate innate and acquired immunity to infection. *Exp. Parasitol.* **84**, 231–244.

ANDRADE S. (1990) Influence of *Trypanosoma cruzi* strain on the pathogenesis of chronic myocardiopathy in mice. *Mem. Inst Oswaldo Cruz.* **85**, 17–27.

ARAÚJO-JORGE T.C., SAMPAIO E.P., DE SOUZA W. & MEIRELLES M.N.L. (1989) *Trypanosoma cruzi*: The effect of variations in the experimental conditions on the levels of macrophage infection *in vitro*. *Parasitol. Res.* **75**, 257–263.

BISAGGIO R.C., CASTRO S.L., BARBOSA H.S., BRANDÃO C.A. & PERSECHINI P.M. (1997) *Trypanosoma cruzi:* Resistance to the pore-forming protein of cytotoxic lymphocytes – perforin. *Exp. Parasitol.* **86**, 144–154.

CARDILLO F., VOLTARELLI J.C., REED S.G. & SILVA J.S. (1996) Regulation of *Trypanosoma cruzi* infection in mice by gamma interferon and interleukin 10: role of NK cells. *Infect. Immun.* **64**, 128–134.

COOPER A.M., D'SOUZA C., FRANK A.A. & ORME I.M. (1997) The course of Mycobacterium tuberculosis infection in the lungs of mice lacking expression of either perforin- or granzime-mediated cytolytic mechanisms. *Infect. Immun.* **65**, 1317–1320.

DENKERS E.Y., YAP G., SCHARTON-KERSTEN T. *ET AL.* (1997) Perforin-mediated cytolysis plays a limited role in host resistance to *Toxoplasma gondii*. *J. Immunol.* **159**, 1903–1908.

DUKE R.C., PERSECHINI P.M., CHANG S., LIU C.-C., COHEN J.J. & YOUNG J.D.E. (1989) Purified perforin induces target cell lysis but not DNA fragmentation. *J. Exp. Med.* **170**, 1451–1456.

FRANCO M.A., TIN C., ROTT L.S., VANCOTT J.L., MCGHEE J.R. & GREENBERG H.B. (1997) Evidence for $CD8^+$ T-cell immunity to murine rotavirus in the absence of perforin, Fas, and gamma interferon. *J. Virol.* **71**, 479–486.

DA COSTA S.C.G., CALABRESE K.S., BAUER P.G., SAVINO W. & LAGRANGE P.H. (1991) Studies of the thymus in Chagas' disease III. Colonization of the thymus and other lymphoid organs of adult and newborn mice by *Trypanosoma cruzi*. *Path. Biol.* **39**, 91–97.

HENRIQUES-PONS A., CORREA A.F.S., BATISTA M.M. *ET AL.* (1998) Perforin knock-out mice infected with a highly virulent strain of *Trypanosoma cruzi* have normal patterns of parasitaemia but higher mortality rates and myocarditis. 10th International Cong. Immunology, New Delhi, India. eds. G.P. Talwar, I. Nath, N.K. Ganguly and K.V.S. Rao, Bologna: *Monduzzi Ed.* **2**, 1007–1010.

KÄGI D., LEDERMANN B., BÜRKI K., HENGARTNER H. & ZINKERNAGEL R.M. (1994) $CD8^+$ T cell-mediated protection against an intracellular bacterium by perforin-dependent cytotoxicity. *Eur. J. Immunol.* **24**, 3068–3072.

KÄGI D., ODERMATT B. & MAK T.W. (1999) Homeostatic regulation of $CD8^+$ T cells by perforin. *Eur. J. Immunol.* **29**, 3266–3272.

KÄGI D., SEILER P., PAVLOVIC J. *ET AL.* (1995) The roles of perforin- and Fas-dependent cytotoxicity in protection against cytopathic and noncytopathic viruses. *Eur. J. Immunol.* **25**, 3256–3262.

KUMAR S. & TARLETON R.L. (1998) The relative contribution of antibody production and $CD8^+$ T cell function to immune control of *Trypanosoma cruzi*. *Parasite Immunol.* **20**, 207–216.

LIU C.-C., WALSH C.M. & YOUNG J.D.-E. (1995) Perforin: structure and function. *Immunol. Today.* **16**, 194–201.

MATLOUBIAN M., SUREESH M., GLASS A. *ET AL.* (1999) A role for perforin in downregulating T-cell responses during chronic viral infection. *J. Virol.* **73**, 2527–2536.

MELINO G., CATANI M.V., GUERRIERI P. & BERNASSOLA F. (2000) Nitric Oxide can inhibit apoptosis or switch it into necrosis. *Cell. Mol. Life Sci.* **57**, 612–622.

MINOPRIO P.M., EISEN H., FORNI L., LIMA M.R.D., JOSKOWICZ M. & COUTINHO A. (1991) Polyclonal lymphocyte responses to murine *Trypanosoma cruzi* infection. I. Quantification of both T- and B-cell responses. *Scand. J. Immunol.* **24**, 661–668.

MORRIS S.A., TANOWITZ H.B., WITTNER M. & BILEZIKIAN J.P. (1990) Pathophysiological insights into the cardiomyopathy of Chagas' disease. *Circulation* **82**, 1990–1909.

MOTYKA B., KORBUTT G., PINKOSKI M.J. *ET AL.* (2001) Mannose 6-phosphate/insulin-like growth factor II receptor is a death receptor for granzyme B during cytotoxic T cell-induced apoptosis. *Cell* **103**, 491–500.

NAKAJIMA H. & HENKART P.A. (1994) Cytotoxic lymphocyte granzymes trigger a target cell internal disintegration pathway leading to cytolysis and DNA breakdown. *J. Immunol.* **152**, 1057–1063.

NICKELL S.P. & SHARMA D. (2000) *Trypanosoma cruzi*: roles for perforin-dependent and perforin-independent immune mechanisms in acute resistance. *Exp. Parasitol.* **94**, 207–216.

PINKOSKI M.J., HOBMAN M., HEIBEIN J.A. *ET AL.* Entry and trafficking of granzyme B., in target cells during granzyme B. and -perforin-mediated apoptosis. *Blood.* **92**, 1044–1054.

PULKKI K.J. (1997) Cytokines and cardiomyocyte death. *Ann. Med.* **29**, 339–343.

REED S.G. (1998) Immunology of *Trypanosoma cruzi* infections. *Chem. Immunol. Basel. Karger.* **70**, 124–143.

ROSSI M.A. & BESTETTI R.B. (1995) The challenge of chagasic cardiomyopathy. *Cardiology* **86**, 1–7.

ROSSI M.A. & SILVA J.S. (1990) Permeability alteration of the sarcolemmal membrane, particularly at the site of macrophage contact, in experimental chronic *Trypanosoma cruzi* myocarditis in mice. *Inst J. Exp. Pathol.* **71**, 545–555.

ROTTENBERG M.E., RIARTE A., SPORRONG L. *ET AL.* (1995) Outcome of infection with different strains of *Trypanosoma cruzi* in mice lacking CD4 and/or CD8. *Immunol. Lett.* **45**, 53–60.

RUSSO M., STAROBINAS N., MINOPRIO P. *ET AL.* (1988) Parasitic load increases and myocardial inflammation decreases in *Trypanosoma cruzi*-infected mice after inactivation of helper T cells. *Ann. Inst Pasteur Immunol.* **139**, 225–236.

SAMBHARA S., SWITZER I., KURICHH A. *ET AL.* (1998) Enhanced antibody and cytokine responses to influenza viral antigens in perforin-deficient mice. *Cell. Immunol.* **187**, 13–18.

SCHARTON-KERSTEN T. & SCOTT P. (1995) The role of the innate immune response in Th1 cell development following *Leishmania major* infection. *J. Leuk. Biol.* **57**, 515–522.

SCHMUNIS G.A., CAPPA S.M.G., TRAVERSA O.C. & JANOVSKY J.F. (1971) The effect of immuno-depression due to neonatal thymectomy on infections with *Trypanosoma cruzi* in mice. *Trans. R. Soc. Trop. Med. Hyg.* **65**, 89–94.

SHIMOJO T., HIROE M., ISHIYAMA S., ITO H., NISHIKAWA T. & MARUMO F. (1999) Nitric oxide induces apoptotic death of cardiomyocytes via a cyclic-GMP-dependent pathway. *Exp. Cell. Res.* **247**, 38–47.

SOUZA A.P., OLIVIERI B.P., DE CASTRO S.L. & ARAÚJO-JORGE T.C. (2000) Enzymatic markers of heart lesions in mice infected with *Trypanosoma cruzi* and submitted to benznidazole chemotherapy. *Parasitol. Res.* **86**, 800–808.

SPANER D., KALIANNAN R., RABINOVICH B. & MILLER R.G. (1999) A role for perforin in activation-induced T cell death *in vivo*: increased expansion of allogeneic perforin-deficient T cells in SCID mice. *J. Immunol.* **162**, 1192–1199.

SPIELMAN J., LEE R.K. & PODACK E.R. (1998) Perforin/Fas-Ligand double deficiency is associated with macrophage expansion and severe pancreatitis. *J. Immunol.* **161**, 7063–7070.

STEPP S.E., MATHEW A.P., BENETT M., SAINT BASILE G. & KUMAR V. (2000) Perforin: more than just an effector molecule. *Immunol. Today.* **21**, 254–256.

TARLETON R.L. (1990) Depletion of $CD8^+$ T cells increases susceptibility and reverses vaccine-induced immunity in mice infected with *Trypanosoma cruzi*. *J. Immunol.* **144**, 717–724.

TARLETON R.L., KOLLER B.H., LATOUR A. & POSTAN M. (1992) Susceptibility of β_2-microglobulin-deficient mice to *Trypanosoma cruzi* infection. *Nature.* **356**, 338–340.

TRAPANI J.A., JANS D.A., JANS P.J., SMYTH M.J., BROWNE K.A. & SUTTON V.R. (1998) Efficient nuclear targeting of granzyme B and the nuclear consequences of apoptosis induced by granzyme B and perforin are caspase-dependent, but cell death is caspase-independent. *J. Biol. Chem.* **273**, 27934–27938.

UNDP/WORLD BANK/WHO SPECIAL PROGRAMME FOR RESEARCH AND TRAINING IN TROPICAL DISEASE (1997) *Tropical Disease Research (TDR), Thirteenth Programme Report*. Geneva: UNDP/WORLD BANK/WHO; pp. 113–123.

VAN DEN BROEK M.F., KÄGI D., OSSENDORP F. *ET AL.* (1996) Decreased tumor surveillance in perforin-deficient mice. *J. Exp. Med.* **184**, 1781–1790.

WALKER W., ROBERTS C.W., FERGUSON D.J.P., JEBBARI H. & ALEXANDER J. (1997) Innate immunity to *Toxoplasma gondii* is influenced by Gender and is associated with differences in interleukin-12 and gamma interferon production. *Infect. Immun.* **65**, 1119–1121.

WALSH C.M., HAYASHI F., SAFFRAN D.C., JU S., BERKE G. & CLARK W.R. (1996) Cell-mediated cytotoxicity results from, but may not be critical for, primary allograft rejection. *J. Immunol.* **156**, 1436–1441.

WALSH C.M., MATLOUBIAN M., LIU C.-C. *ET AL.* (1994) Immune function in mice lacking the perforin gene. *Proc. Natl. Acad. Sci.* **91**, 10854–10858.

YOUNG J.D.-E., COHN Z.A. & PODACK E.R. (1986) The ninth component of complement and the pore-forming protein (perforin I) from cytotoxic T cells: structural, immunological and functional similarities. *Science.* **233**, 184–190.